



HHS Public Access

Author manuscript

Nat Immunol. Author manuscript; available in PMC 2014 September 11.

Published in final edited form as:

Nat Immunol. 2013 April ; 14(4): 364–371. doi:10.1038/ni.2541.

STAT5 is critical in Dendritic Cells for development of T_H2- but not T_H1-dependent Immunity

Bryan D. Bell^{1,2,6}, Masayuki Kitajima^{1,2,6}, Ryan P. Larson^{1,2}, Thomas A. Stoklasek^{1,2}, Kristen Dang¹, Kazuhito Sakamoto³, Kay-Uwe Wagner³, Boris Reizis⁴, Lothar Hennighausen⁵, and Steven F. Ziegler^{1,2}

¹Immunology Program, Benaroya Research Institute at Virginia Mason, Seattle, WA98101

²Department of Immunology, University of Washington School of Medicine, Seattle, WA98195

³Eppley Institute for Research in Cancer and Allied Diseases, University of Nebraska Medical Center, 985950 Nebraska Medical Center, Omaha, Nebraska 68198-5950, USA

⁴Department of Microbiology and Immunology, Columbia University Medical Center, New York, NY 10032

⁵Laboratory of Genetics and Physiology, National Institutes of Health, Bethesda, MD, USA.

Abstract

Dendritic cells (DCs) are a critical player in immune responses, linking innate and adaptive immunity. We show here that DC-specific deletion of the STAT5 was not critical for development, but was required for type-2, but not type-1, allergic responses in both the skin and lung. Loss of STAT5 in DCs led to the inability to respond to thymic stromal lymphopoietin (TSLP). STAT5 was required for TSLP-dependent DC activation, including upregulation of costimulatory molecules and chemokine production. Furthermore, type-2 responses in mice with DC-specific loss of STAT5 resembled those seen in TSLPR-deficient mice. These results show that the TSLP- STAT5 axis in DCs is a critical component for the promotion of type-2 immunity at barrier surfaces.

Keywords

TSLP; Dendritic Cell; Contact Hypersensitivity; Stat5

Users may view, print, copy, download and text and data- mine the content in such documents, for the purposes of academic research, subject always to the full Conditions of use: http://www.nature.com/authors/editorial_policies/license.html#terms

Correspondence should be addressed to S.F.Z. (sziegler@benaroyaresearch.org), Steven F. Ziegler, Benaroya Research Institute at Virginia Mason, 1201 Ninth Avenue, Seattle WA 98101, Telephone: 206-287-5657, Fax: 206-342-6572.

⁶These authors contributed equally to the work in this manuscript

Author contributions? B. D. B and M. K. performed most of the experiments and wrote the manuscript, with help from S. F. Z. K. S., K-U. W., B. R., and L. H. provided strains and expertise for these studies. R. P. L. collaborated on the contact hypersensitivity studies, and T. A. S. performed the influenza infections and did the analysis of the response to infection. K. D. provided help with bioinformatics. S. F. Z. supervised all of the work in this study.

Introduction

Three cytokine pathways have been identified as important for DC development both *in vivo* and *in vitro*. Of these, only Flt3L appears to be non-redundant as deletion of Flt3L reduces the number of DCs by 90%^{1, 2}. The failure of DC development in Flt3L-deficient mice appears to be due to lack of STAT3 activation³. Further support for the importance of STAT3 in DC development comes from studies using ectopic expression of STAT3 in non-DC hematopoietic progenitors resulted in development of both cDCs and pDCs⁴. However, the influence of STAT3 may be restricted to Flt3 signaling as *in vitro* DC differentiation driven by GM-CSF is unaffected by STAT3 deficiency³

A similar non-redundant role for STAT5 in DC development is less clear. GM-CSF can activate both STAT5 and STAT3 and GM-CSF-activated STAT5 inhibits the transcription of *Irf8* (ref. ⁵), encoding a transcription factor previously shown to be critical for pDC and CD8 α^+ cDC development *in vivo*⁶. In addition GM-CSF-activated STAT5 also inhibited Spi-B, Irf-7, Flt3 and TLR9, all factors involved in pDC development^{1, 7}. Thus, one potential role for STAT5 is to promote cDC differentiation through inhibition of pDC development.

Following maturation, multiple cytokines have been shown to activate STAT5 in DCs, including GM-CSF and thymic stromal lymphopoietin (TSLP). TSLP is expressed by a variety of cell types and signals via a heterodimer of interleukin 7 receptor α (IL-7R α) and the unique TSLP receptor (TSLPR) chain^{8, 9}. IL-7R α and TSLPR utilize the signaling kinases Jak-1 and Jak-2, respectively, for the activation of signal transducer and activator of transcription (STAT) proteins in human DCs and murine CD4⁺ T lymphocytes^{10, 11}. In human DCs, TSLP has been shown to activate STAT-1, -3, -4, -5 and -6 (ref.¹¹). Mouse studies showed that TSLP stimulation lead to the activation of STAT5 and induction of STAT5 responsive genes¹²⁻¹⁶.

Several cell types have been shown to be TSLP-responsive, including DCs, Langerhans cells, T cells, B cells, basophils, eosinophils and monocyte/macrophages⁸. *In vivo* studies have shown that both DCs and CD4⁺ T cells are important for TSLP-dependent responses¹⁷⁻¹⁹. Furthermore, elevated concentrations of TSLP are associated with allergic diseases in humans and are important for type 2 inflammatory responses in mice^{8, 20}.

We tested the consequence of CD11c-cre mediated deletion of STAT5 on DC homeostasis and multiple TSLP-dependent and independent T_H2 and T_H1 responses *in vivo*, respectively. Here, we show that STAT5 is dispensable for normal DC homeostasis and function, but is absolutely required for multiple models of TSLP-dependent T_H2-mediated atopic disorders. Importantly, T_H1 responses in mice that lack STAT5 in DCs is normal. The T_H2 defects are due to multiple factors, including reduced migration and activation of antigen-bearing DCs following sensitization, and concomitant reduction in the ability to drive antigen-specific T cell proliferation and T_H2 cytokine production. Together, this highlights the importance of STAT5 in DCs during TSLP-mediated T_H2 responses, and suggests that DCs are a critical *in vivo* target of TSLP.

Results

STAT5 is not required for normal DC homeostasis

To test the requirement for STAT5 in DCs to promote T_H1 and T_H2 immune responses, we first measured the consequences of CD11c-Cre-mediated deletion of *Stat5*^{fl/f} in spleens of CD11c-Cre⁻ × *Stat5*^{fl/f} (Cre^{-5fl/fl}) and CD11c-Cre⁺ × *Stat5*^{fl/f} (Cre^{+5fl/fl}) mice (insert refs 5/20/21). Total cellularity between Cre^{-5fl/fl} and Cre^{+5fl/fl} mice was similar, along with percentages of NK cells, macrophages, neutrophils and lymphocytes (Supplementary Fig. 1a). Three major populations of DCs exist in the spleen; pDCs (CD11c⁺CD11b⁻PDCA1⁺), CD8⁺ DCs (CD11c⁺CD11b⁻PDCA1⁻CD8α⁺CD4⁻) and CD4⁺ DCs (CD11c⁺CD11b⁺PDCA1⁻CD8⁻CD4⁺). The percentage and absolute numbers of each DC population was similar in Cre^{-5fl/fl} and Cre^{+5fl/fl} spleens (Supplementary Fig. 1b). Lineage tracing studies showed that the activity of CD11c-Cre (RFP⁺ DCs, open shapes, Supplementary Fig. 1b) correlated with the extent of germline recombination at the *Stat5* locus (Supplementary Fig. 1c). CD8⁺ DCs had the highest efficiency of *Stat5* deletion, while pDCs showed a 50% deletion of *Stat5* in the germline.

We analyzed DC subsets present in the epidermal and dermal layers of skin and skin-draining LNs (skin dLNs) in Cre^{+5fl/fl} mice. Langerhans cells (LCs) constitute a homogenous subset of DCs which reside in the epidermis, and only MHCII^{hi}CD11b⁺CD207(langerin)⁺ LCs were detected in the Cre^{-5fl/fl} and Cre^{+5fl/fl} epidermis (Supplementary Fig. 2 a, b). Four distinct steady-state dermal DC (dDC) subsets have been identified²¹. First, CD207^{hi}CD11b^{int} (R1) corresponds to migratory LCs (mLCs) enroute to the skin dLNs. Secondly, CD207⁺CD11b⁻DC (R2) corresponds to the langerin⁺ dDC subset. Two CD207⁻ dDC subsets, CD11b⁻ and CD11b⁺ (R3 and R4, respectively), were found in the Cre^{-5fl/fl} and Cre^{+5fl/fl} dermis (Supplementary Fig. 2a). The skin dLN DCs are more heterogeneous as they include blood-derived lymphoid-tissue-resident CD4⁺ DCs, CD8⁺ DCs, mLCs and dDCs²². In skin dLNs MHCII, CD207 and CD11b expression does not allow for the discrimination of mLCs and dDCs, as both appear as CD207⁺CD11b^{-/lo} (R1/R2, Supplementary Fig. 2c). Skin dLNs from Cre^{+5fl/fl} mice were consistently smaller than from Cre^{-5fl/fl} mice (Supplementary Fig. 2d). However, numbers for all lymph node cell populations were reduced equally, as the percentages of Cre^{+5fl/fl} LN cell populations were similar to wild-type (Supplementary Fig. 2e and data not shown). Finally, greater than 90% of CD11c⁺ DCs from the skin dLNs were RFP⁺, suggesting efficient CD11c-Cre activity in the Cre^{+5fl/fl} LNs (Supplementary Fig. 2f). In addition, TSLPR expression on epidermal DCs, dermal DCs, and skin LN DCs were equivalent between Cre^{-5fl/fl} and Cre^{+5fl/fl} mice (Supplementary Fig. 2g). Taken together, these data show that the loss of STAT5 in CD11c⁺ cells does not preclude the development of any DC subset in the spleen, skin, lung or LNs, and only affects the total cellularity of LNs. Furthermore, loss of STAT5 does not lead to overt autoimmune pathology that was seen in mice where STAT3 is specifically deleted in DCs⁽²³⁾ and data not shown).

Promotion of Th2 CHS requires STAT5 in Dermal DCs

Contact hypersensitivity (CHS) is an animal model for human allergic contact dermatitis Gober, 2008 2734 /id}. It is divided into two distinct phases, sensitization and elicitation, the

latter occurring following antigen exposure to a previously unexposed site. The hapten fluorescein isothiocyanate (FITC), in combination with dibutyl phthalate (DBP), induces a T_H2-type response in mice^{24, 25}. To understand the role of STAT5 in DCs during a T_H2 response, wild-type and Cre^{+5^{fl/fl}} mice were sensitized and challenged with FITC-DBP. Ear swelling 24 h following challenge was markedly reduced in Cre^{+5^{fl/fl}} mice compared to wild-type mice (Fig. 1a). Correspondingly, wild-type mice displayed a substantial cellular infiltrate, epidermal thickening and lesions, which were markedly reduced in challenged Cre^{+5^{fl/fl}} mice (Fig. 1b). Mice which lacked STAT5 in DCs had reduced IL-4 mRNA in the inflamed ears (Fig. 1c). In addition, the percentage of BrdU⁺ and CD44^{hi}CD4⁺ T cells in the skin dLN was reduced in Cre^{+5^{fl/fl}} mice, suggesting an inability of STAT5-deficient DCs to activate antigen-specific T cells (Fig. 1d). We further observed a significant reduction in the number of FITC⁺ DCs in the skin dLNs and the expression of CD86 on FITC⁺ DCs from Cre^{+5^{fl/fl}} mice, suggesting a possible mechanism for the reduction in CD4⁺ T cell proliferation (Fig. 1e).

To test whether the lack of response in the FITC-DBP model was due to a general DC defect we utilized a second CHS model known to induce a T_H1 response by sensitization and challenge with the hapten 2,4-dinitrofluorobenzene (DNFB)²⁶. In both wild-type and Cre^{+5^{fl/fl}} mice, DNFB CHS lead to significant ear-swelling (Fig. 2a). Furthermore, while the cellularity of steady-state skin dLNs of Cre^{+5^{fl/fl}} mice was consistently smaller, the fold-increase in cellularity between DNFB-treated wild-type and Cre^{+5^{fl/fl}} mice was not significantly different (Fig. 2b). There was also no difference in IFN- γ and IL-17 mRNA, CD4⁺ and CD8⁺ T cell proliferation and CD44 expression in challenged wild-type and Cre^{+5^{fl/fl}} mice (Fig. 2c, d).

During sensitization, both LC and dermal DCs endocytose uptake hapten-protein complexes and migrate to skin dLNs. To determine if loss of a T_H2 CHS response is due to the absence of STAT5 in Langerhans cells or dermal DCs, we crossed human Langerin-Cre and *Stat5^{fl/fl}*(Lang-Cre^{+5^{fl/fl}}) mice. Use of human Langerin-Cre restricts expression to mouse Langerhans cells²⁷. Loss of STAT5 in LCs did not affect the number or distribution of LCs in the epidermis or mLCs in the dermis (Fig. 3a, b). Following sensitization and challenge with FITC-DBP, Lang-Cre^{+5^{fl/fl}} had similar ear swelling, as well as other aspects of the response, compared to wild-type and Lang-Cre^{-5^{fl/fl}} controls (Fig. 3c, d). Taken together, this shows that STAT5 is required in dDC subsets for control of T_H2 skin responses.

Th2-dependent lung responses require STAT5 in DCs

To understand if STAT5 in DCs is generally required for Th2-type inflammation, we used two models of airway inflammation. First, we tested the requirement for STAT5 in DCs during ovalbumin (OVA)-induced airway inflammation²⁸. On day 10, as expected, wild-type mice had a significant increase in BAL cellularity, which was primarily eosinophilic and characterized by type-2 cytokine production (Fig. 4a, b). However, Cre^{+5^{fl/fl}} mice recruited fewer eosinophils, produced less IL4, and increased IFN- γ , compared to wild-type mice (Fig. 4a, b).

To determine whether the absence of STAT5 in CD11c⁺ DCs leads to an inability of the mice to respond to general lung inflammation, we infected mice with influenza A virus

(IAV). Infection with IAV is dominated by proinflammatory and T_H1-associated cytokines. Wild-type and Cre^{+5^{fl/fl}} mice were infected with IAV (A/Aichi/68 (H3N2)) and, as expected, wild-type mice lost weight, but began to recover after 5 days, similar to Cre^{+5^{fl/fl}} mice (Fig. 4c). We saw no differences in the total cell numbers of the BAL, man or lung cells, as well as no difference in the percentage or number of CD4⁺ and CD8⁺ T cells present in these sites at day 8 (data not shown). We found that the immunodominant lung CD8⁺ T cell response was similar in wild-type and Cre^{+5^{fl/fl}} mice (Fig. 4d). No difference was noted in the size of the total memory-activated CD8⁺ T cell compartment (CD44^{hi} CD11a^{hi}) (data not shown). As seen with the CD8⁺ T cell tetramer response, the number of lung CD4⁺ T cells capable of producing IFN- γ after *in vitro* restimulation was unchanged in the Cre^{+5^{fl/fl}} mice (Fig. 4e). Thus, the T_H1 and cytolytic T cell response to IAV appears intact in the Cre^{+5^{fl/fl}} mice. Altogether, this suggests that DCs require STAT5 for the development and promotion of T_H2 responses in the lung, while T_H1 responses are independent of STAT5.

Lack of *in vivo* TSLP responses in Cre^{+5^{fl/fl}} mice

Since DC development is unperturbed in Cre^{+5^{fl/fl}}, we hypothesized that during a T_H2 response STAT5-inducing cytokine(s) would be critical for DC activation. We examined mRNA expression of three STAT5-activating cytokines 24 h after FITC-DBP exposure (Supplementary Fig. 3a and ¹⁹). The four-fold increase in TSLP mRNA is consistent with the lack of an inflammatory response to FITC-DBP sensitization and challenge in *Tslpr*^{-/-} mice²³. Thus, in both T_H2 skin and lung antigen-driven models tested, the absence of STAT5 in DCs phenocopies what is seen in the absence of the TSLPR, suggesting that DCs are the *in vivo* target of TSLP.

To test this hypothesis directly we used a model of acute airway inflammation utilizing intranasal administration of TSLP and antigen, leading to a marked increase in T_H2-type airway inflammation (Supplementary Fig. 4a and ²⁹). As seen in TSLPR-deficient animals, Cre^{+5^{fl/fl}} mice had no significant change in either BAL cell count or eosinophil recruitment (Supplementary Fig. 4a, b). Intracellular cytokine signaling of CD4⁺ T cells from mLN showed a reduction in both IL-4 and IL-13 in Cre^{+5^{fl/fl}} mice (Supplementary Fig. 4c). Expression of CCL17 and IL-4 mRNA was significantly reduced in Cre^{+5^{fl/fl}} lungs, as well as serum IgE, compared to wild-type (Supplementary Fig. 4d, e). Each of these findings further supports our hypothesis that TSLP activates STAT5 in DCs in both the skin and lung to promote T_H2 immunity.

Role of STAT proteins in TSLP-mediated DC maturation

Previous work has shown that BMDCs generated using either GM-CSF or Flt3L respond to TSLP, with upregulation of CD80, CD86 and OX40L, and production of CCL17^{28, 30}. Whole FL-DC cultures were left untreated or treated with TSLP for 96 h. There was no change in MHC class II expression, but surface expression of CD80, CD86 and OX40L was increased in TSLP-treated FL-CD11b-DCs, while TSLP had no effect on FL-pDCs or FL-CD24-DCs (Supplementary Fig. 5a). The time course revealed that CD80 and CD86 were maximally expressed at 48 h, while OX40L expression peaked at 72 h, similar to human peripheral blood CD11c⁺ DCs³¹. TSLP treatment of GM-DCs similarly leads to increased expression of CD86 and OX40L (Supplementary Fig. 5b). To determine whether TSLP

signaling in the FL-DCs mimicked the primary DC subsets they represent, we tested the effect of TSLP on splenic pDCs, CD4⁺ DCs and CD8⁺ DCs *ex vivo*. Similar to FL-CD11b-DCs, only CD4⁺ splenic DCs had significant increases in CD80 and CD86 expression in response to TSLP. However, this increase was more transient than in the FL-CD11b-DCs, as CD80 and CD86 expression increased at 24 h, but was not significantly increased at 48 h post-TSLP treatment (Supplementary Fig. 5c). These data suggest that TSLP exerts these effects on specific DC subsets.

TSLP-induced Jak-STAT5 signaling in DCs

Recent studies have found that TSLP can activate Jak1 and Jak2 in human DCs^{10, 11}. The three FL-DC populations were treated with TSLP, IL-7 (activates Jak1) and IL-6 (activates Jak2) for 5 min, which led to the activation of both Jak1 and Jak2 in FL-CD11b-DCs, but not in FL-pDCs or FL-CD24-DCs (Supplementary Fig. 6a and data not shown). To directly test the role of Jak2, we generated FL-DCs from *Jak2^{fl/fl}* mice and infected them with a retrovirus expressing Cre recombinase, with a GFP marker, to delete *Jak2*. Uninfected and sorted GFP⁻ and GFP⁺ infected *Jak2^{fl/fl}* FL-CD11b-DCs were stimulated with TSLP, IL-7 and IL-4. CCL17 expression was used as a readout of TSLP signaling as CCL17 is a direct TSLP target gene^(28 and M.K. and S.F.Z., manuscript in preparation). GFP⁺ FL-CD11b-DCs stimulated with IL-7 or IL-4 had a 2-fold reduction in CCL17 production compared to GFP⁻ and wild-type controls, while loss of Jak2 led to a 10-fold reduction in CCL17 production following TSLP treatment (Supplementary Fig. 6b). In addition, the absence of Jak3 had no effect on STAT5 phosphorylation following TSLP treatment when compared to wild-type FL-CD11b-DCs (data not shown). This data shows that murine DCs can utilize Jak-1 and Jak-2 to propagate TSLP signals.

In human myeloid DCs, TSLP was shown to activate STAT-1, -3, -4, -5, and -6, although the contributions of the individual STATs in DC activation are still unclear^{10, 11, 32}. We checked for phosphorylated STATs in all FL-DC populations, and as expected, TSLP treatment of FL-DC subsets led to phosphorylated STAT5 only in FL-CD11b-DCs (Fig. 5a), although FL-pDCs and FL-CD24-DCs were capable of activating STAT-1, -3, -5 and -6 with IFN- α , GM-CSF, GM-CSF and IL-4, respectively (data not shown). We also measured the protein abundance of SOCS-1, -2, and -3 in all three Flt3L BMDC populations to determine whether differential SOCS expression could account for the absence of Jak-STAT signaling in the FL-pDCs and FL-CD24-DCs. Protein expression of SOCS-1, -2 and -3 were similar in all three FL-DC populations (data not shown). Because STAT5 mediates TSLP-dependent proliferation and transcription of target genes in multiple cell lines, we tested the requirement for STAT5 in TSLP-driven DC maturation^{10, 12, 14}. We confirmed that STAT5 is dispensable for FL-DC development and was efficient in all FL-DC populations (Fig. 5b, c, data not shown and 5). The loss of STAT5 in FL-CD11b-DCs correlated with a reduction in TSLP-induced CD80, CD86 and OX40L upregulation (Fig. 5d). The residual upregulation of costimulatory molecules was not due to compensatory STAT upregulation, as no increases in phosphorylation of STAT-1, -3, -4 or -6 was seen in Cre⁺5^{fl/fl} FL-DCs (Fig. 5a). The loss of co-receptor upregulation was not due to a developmental defect in Cre⁺5^{fl/fl} DCs, as LPS induced similar expression of CD80 and CD86 compared to Cre⁻5^{fl/fl} (Fig. 5f). The absence of the STAT-1, -4, -5 or -6 did not affect the generation of the three FL-DC

subsets (data not shown). Thus only loss of STAT5 affected upregulation of CD80, CD86 and OX40L in response to TSLP (Fig.5e).

To test which STAT controls CCL17 production in response to TSLP, we obtained a mouse strain that contains the gene encoding GFP targeted to the endogenous *Ccl17* locus (CCL17-eGFP)³³. As expected, untreated heterozygous CCL17-eGFP FL-DCs did not produce CCL17, while TSLP stimulation led to detection of GFP⁺CD11c⁺ FL-DCs, and the GFP was confined to the FL-CD11b-DC population (data not shown). While there was no defect in CCL17 production in DCs lacking STAT-1, -4 or -6, the loss of STAT5 severely impaired CCL17 expression following TSLP treatment (Fig.5g). Thus, TSLP-induced CCL17 production in murine DCs is STAT6 independent. Together, this data shows that TSLP activates STAT5 in FL-CD11b-DCs, and that STAT5 activation is required for the complete upregulation of costimulatory molecules and CCL17 production by FL-CD11b-DCs.

STAT5 activation by TSLP promotes Th2 signal in DCs

The cumulative effect of TSLP-induced costimulatory molecule upregulation and chemokine production on DCs is the inflammatory T_H2 phenotype adopted by CD4⁺ T cells primed by these DCs²⁰. To test whether DC-specific STAT5 is required for this process, wild-type and Cre^{+5^{fl/fl}}FL-CD11b-DCs were cultured with TSLP overnight, and then pulsed with OVA peptide and co-cultured with CFSE-labeled naïve DO11.10 CD4⁺ T cells. Untreated DCs generated from wild-type and Cre^{+5^{fl/fl}} bone marrow led to similar CFSE dilution profiles by activated CD4⁺ T cells, while wild-type, but not STAT5-deficient, DCs promoted enhanced proliferation following TSLP treatment (data not shown). Accordingly, T_H2 cytokine induction was significantly reduced when CD4⁺T cells were co-cultured with TSLP-treated Cre^{+5^{fl/fl}} DCs compared to wild-type (Fig.6a). Furthermore, only wild-type TSLP-treated DCs were able to reduce the expression of IFN- γ by the activated CD4⁺ T cells. Similar results were obtained using TSLPR-deficient DO11.10 T cells (data not shown). Lastly, we tested the ability of Cre^{+5^{fl/fl}} DCs to promote CD4⁺ T cell expression of IFN- γ and IL-4 in neutral, T_H1- and T_H2-skewing conditions compared to wild-type DCs. When the DCs were not pretreated with TSLP, similar numbers of IFN- γ ⁺ and IL-4⁺ CD4⁺ T cells were generated under neutral, T_H1- and T_H2-skewing conditions (Fig.6b,c). These data show that FL-CD11b-DCs that lack STAT5 are capable of generating both T_H1 and T_H2 cells under appropriate conditions, and the defect in T_H2 cell activation only occurs in the absence of STAT5 in TSLP-treated DCs. To test the T cell stimulatory capacity of STAT5-deficient DCs *in vivo*, we transferred CFSE-labeled DO11.10 CD4⁺ T cells into wild-type, Cre^{+5^{fl/fl}} and *Tslpr*^{-/-} hosts. Intradermal injections of OVA in PBS lead to dilution of CFSE and detectable numbers of IL-4⁺ and IL-13⁺ CFSE¹⁰ CD4⁺ T cells in all three hosts, showing dermal DCs lacking STAT5 or TSLPR are capable of migration, antigen processing and presentation to naïve CD4⁺ T cells (Fig.6d, e). Intradermal injection of OVA plus TSLP lead to enhanced T cell proliferation and production of IL-4 and IL-13 in wild-type hosts (Fig.6d,e). This enhancement of T_H2 cytokine production in the presence of antigen and TSLP was lost in the Cre^{+5^{fl/fl}} and *Tslpr*^{-/-} hosts. Consistent with the *in vitro* data, DCs require STAT5 *in vivo* for TSLP-mediated T_H2 differentiation.

Discussion

We cannot determine from these data whether STAT5 is critical for DC development as CD11c is expressed late in development³⁴. However, it is clear that STAT5 is dispensable for DC homeostasis. This finding differs from previous work that found STAT5 deficiency led to a decrease in the number of cDCs⁵. In that study, fetal liver cells from wild-type and STAT5-deficient mice were used to reconstitute lethally-irradiated hosts, and the reconstituted animals in this study were immunodeficient, impacting splenic architecture and DC numbers⁵. In the studies shown here, STAT5 is only deleted in cells that express CD11c, and the only discernible difference we have found is reduced lymphoid- and myeloid-lineage cellularity in LNs. When STAT5 deletion is restricted to LCs LN cellularity remains at WT levels, suggesting that the defect only arises when dermal and/or LN-resident DCs lack STAT5. Therefore we feel that this model provides a more accurate picture of the role of STAT5 in DC in homeostasis and survival, and DCs do not require STAT5 for their homeostasis.

Our data are both similar and distinct from a study using CD11c-Cre to delete STAT3 in DCs, as cDC development was largely unaffected²³. However, they found a 50% decrease in splenic and bone marrow pDC numbers, while we did not. The striking difference between the two sets of animals is the development of lymphadenopathy and ileocolitis in the CD11c-Cre/Stat3^{fl/fl} mice²³. This phenotype was attributed to an increase in the activation state of the DCs in these mice. We have analyzed aged Cre⁺Stat5^{fl/fl} mice and have not found any obvious indication of spontaneous inflammation (data not shown). These data suggest different cell-intrinsic roles for STAT3 and STAT5 in DCs homeostasis following CD11c-cre-mediated deletion.

We have shown that there is a specificity of the deficit in DCs from the Cre⁺Stat5^{fl/fl}. In general, the mice have no overt signs of pathology, suggesting that DC function is normal, as either constitutive or conditional DC ablation leads to systemic inflammation and autoimmunity^{35, 36}. In addition, we have shown that DCs from these mice are capable of promoting both Th1- and Th2-type differentiation in an antigen-driven *in vitro* system. In addition, the mice retain normal Th1 responses to DNFB and Influenza virus infection, showing the maintenance of DC function; including antigen acquisition, trafficking, T cell activation and cytokine production.

The surprising finding of the study is the specificity of the defect for Th2 responses *in vivo* in the absence of STAT5 in DCs, as shown by lack of response to the Th2 hapten FITC and Th2-type allergic responses in the lung. The requirement for STAT5 in DCs is restricted to dermal DCs, as Lang-cre/STAT5^{fl/fl} mice respond normally to FITC/DBP. In order to determine the root cause of this defect, we tested for the production of STAT5 activating cytokines, and found TSLP is strongly upregulated following sensitization with FITC (Th2), but not DNFB (Th1).¹⁹ In a wide variety of model systems increased expression of TSLP has led to the induction of type 2 inflammation. We and others have shown a critical role for TSLP in driving antigen-induced airway inflammation in the mouse^{17, 28, 29}. Elevated expression of TSLP in the skin leads to the development of an atopic dermatitis-like disease³⁷⁻⁴⁰. Furthermore, TSLPR deficient mice exhibit a dramatically reduced response

in a Th2 model of contact hypersensitivity¹⁹. We have extended these results to show that in the presence of antigen and TSLP alone, STAT5 was required in DCs for the development of the response. These data, along with the dramatically reduced response of the Cre^{+5^{fl/fl}} mice in the OVA-induced allergy model, are consistent with Stat5 as a critical downstream mediator of TSLPR signals in DCs.

As stated above, human myeloid DCs activated by TSLP phosphorylate multiple STAT proteins¹¹. Only STAT5 is phosphorylated following TSLP stimulation, which is restricted to the FL-CD11b-DCs. STAT5 appears to control all of the TSLP-mediated effects, as the absence leads to reduced CD80, CD86 and OX40L upregulation. Unlike human DCs, the production of CCL17 following TSLP stimulation requires only STAT5.

It is unclear at this point why the FL-CD24-DCs and FL-pDC subsets do not activate STAT5 in response to TSLP, as we have found equivalent levels of IL7Ra and TSLPR on the surface of these DCs (data not shown). One possibility is the presence of yet identified inhibitory molecules, as we found no differences in SOCS-1, -2 or -3 protein expression (data not shown). To understand the specificity of TSLPs actions on a specific DC subsets (FL-CD11b-DCs and GM-DCs), we performed microarray analysis on WT, Cre^{+5^{fl/fl}} and TSLPR deficient FL-DCs. We found that TSLP did indeed cause changes in multiple targets in the FL-pDCs and FL-CD24-DCs subsets (data not shown). We also found that within FL-CD11b-DCs, the absence of STAT5 did not affect approximately 15% of the TSLP-responsive genes, suggesting other signaling pathways are activated downstream of the TSLPR (data not shown).

The importance of TSLP in the initiation and progression of allergic disease is becoming clear. What is less clear are the identity of the key TSLP-responsive cells at sites of disease, and the nature of the signaling pathways employed by those cells to respond to the cytokine. Taken as a whole, our data suggest a model by which STAT5 specifically mediates TSLP responses in DCs following antigen acquisition in the periphery.

Methods

Animals

Six- to twelve-week-old female BALB/c mice, JAK3-deficient and STAT6-deficient mice were purchased from Taconic Farms and Jackson Laboratory. ROSA Stop Flox RFP⁴¹ and bacterial artificial chromosome transgenic *Cd11c*-Cre mice³⁴ were backcrossed 10 generations onto the BALB/c background and then crossed to floxed *Stat5* mice on BALB/c background⁴². Langerin-Cre mice were kindly provided by D. Kaplan (University of Minnesota⁴³). Floxed *Jak2* on BALB/c background. STAT1-deficient on BALB/c background were purchased from Taconic, and backcrossed to BALB/c greater than 10 generations. STAT4-deficient mice on BALB/c background were purchased from Jackson Laboratory. OVA-specific TCR $\alpha\beta$ (DO11. 10) transgenic (Tg) mice were purchased from Jackson Laboratory^{44, 44}. CCL17-eGFP Tg mice on BALB/c background were from by I. Förster³³. All mice for this study were maintained under pathogen-free conditions. All animal procedures were performed in accordance with IACUC guidelines at the Benaroya Research Institute.

Flow Cytometry Analysis

In general, 1×10^6 cells were stained with antibodies. For surface staining, the Abs, PE-Cy7-conjugated anti-CD11c mAb (N418), Biotin-conjugated anti-TSLPR mAb (22H9)¹⁴, PE-conjugated anti-IL-7R α mAb (A7R34), PE-conjugated anti-Fc ϵ R α mAb (MAR-1), Alexa Fluor 647-conjugated anti-CD80 mAb (16-10A1), PE-conjugated anti-CD86 mAb (PO3.1), PE-conjugated anti-OX40L mAb (RM134L), FITC-conjugated anti-I-A^d mAb (AMS-32.1), Pacific blue-conjugated anti-CD11b mAb (M1/70), Alexa Fluor700-conjugated anti-CD8 α mAb (53-6.7), Alexa Fluor780-conjugated anti-CD4 mAb (RM4-5), and PE-conjugated anti-CD103 mAb (2E7), FITC-conjugated anti-B220 mAb (RA306B2), Pacific blue-conjugated anti-CD3 ϵ mAb (145-2C11), Pacific blue-conjugated anti-CD19 mAb (1D3), allophycocyanin-conjugated anti-F4/80 mAb (BM8), PerCP-Cy5.5-conjugated anti-Ly-6C mAb (HK1.4), Pacific blue-conjugated anti-Ly-6G mAb (RB6-8C5), FITC-conjugated anti-mouse DO11.10 TCR mAb (KJ1-26) and allophycocyanin-conjugated streptavidin (eBioscience or BioLegend) were used. For intracellular staining, Alexa Fluor 488-conjugated anti-CD207 mAb (eBioL31), PE-Cy7 anti-IL-4 mAb (BVD6-24G2), and eFlour 450 IFN- γ mAb (XMG1.2) was used. For the phosphorylated STAT intracellular staining, STAT1 (Y701) (4a), STAT3 (Y705) (38/P-STAT3), STAT4 (Y693) (38/p-STAT4), STAT5 (Y694) (47/STAT5(pY694)), STAT6 (Y641) (J71-773.58.11) (BD Biosciences) was used. Cells were run on a BD LSR II flow cytometry using DiVa software or BD FACSCalibur using CellQuest Pro software and sorted on FACS Aria II at 4 °C (BD Biosciences) and analyzed with FlowJo software (Tree Star).

Bone marrow DC cultures

A modified method was used for bone marrow DC cultures as previously described^{5, 45}. In brief, bone marrow cells harvested from femurs and tibias were cultured in the presence of 10 ng/ml murine GM-CSF (Peprotech), with half of media replenished every other day with fresh GM-CSF, for GM-DCs or 200 ng/ml human Flt3L (gift from Amgen) for FL-DCs in RPMI-1640 medium supplemented with 10% FBS, 2-mercaptoethanol, L-glutamine, HEPESpH7.4, sodium pyruvate, MEM non-essential a. a., penicillin and streptomycin (complete RPMI). On day 7–9, the cells were harvested and CD11c⁺ DCs were positively isolated using anti-CD11c mAb-conjugated micro beads and a MACS LS column (Miltenyi Biotech) or DC populations sort purified using a BD FACS Aria II flow cytometer. GM-DCs were sorted into MHCII^{hi}CD11c^{hi}. FL-DCs were sorted into pDCs (B220⁺CD11c⁺), CD11b-DCs (B220-CD11c⁺CD11b^{hi}CD24^{int}) and CD24-DCs (B220-CD11c⁺CD11b⁺CD24^{hi}). The purity was greater than 90% (data not shown). Cells were stimulated with medium alone or medium plus 50 ng/ml of TSLP (gift from Amgen) for indicated times.

Quantitative RT-PCR, DNA deletion and Microarray

Total RNA was isolated from the cells using the GenElute Mammalian Total RNA Kit (SIGMA) or Total RNA was isolated from tissue using TRIzol reagent (Invitrogen), and reverse transcription was performed with Superscript II RT (Invitrogen) according to the manufacturer's protocol. PCR amplification was performed on ABI 7700 Sequence Detector (Applied Biosystems). Quantitative RT-PCR was performed as described with primers to *I14*,

Il17a and *Ifng*^{19, 46}. The expression was normalized by the *Gapdh* signal. The primers used as follows: *Tslpr* forward, 5'-GAGAGCAATGACGATGAGGAC-3'; *Tslpr* Reverse, 5'-GATCTTCCTGCACAGCCAGA-3'; *Il7ra* forward, 5'-GAGAAACTGGTATCAGGATTCCC-3'; *Il7ra* reverse, 5'-GTCTTCAGAGACAGCCAGGA-3'; *Gapdh* forward, 5'-TGCACCACCAACTGCTTAG-3'; *Gapdh* Reverse, 5'-GGATGCAGGGATGATGTTC-3'. The detection of the floxed *Stat5* and deleted *Stat5* in germline DNA was performed as previously described⁴². For microarray, FL-DCs were sorted into CD11b-DCs, CD24-DCs and pDCs, and cells were cultured with medium plus Flt3L (100 ng/ml) overnight, then cells were stimulated with medium alone or TSLP (50ng/ml) for 6 h. Total RNA was isolated from the cells using the RNeasy mini kit according to the manufacturer's instructions (Qiagen) and amplified with Illumina TotalPrep-96 RNA Amplification Kit (Ambion). The resulting cRNA was hybridized to an Illumina MouseWG-6 v2.0 BeadChip (Illumina), and scanned on a HiScan SQ (Illumina) following the manufacturer's protocols. Quality control was performed using an Agilent Bioanalyzer 2100 (Agilent Technologies), and a Tecan Infinite M200 pro Nanoquant (Tecan). Data were normalized and analyzed with the R software.

Retrovirus vectors and infection

pMX-Cre-IRES-GFP were provided by T. Nakayama (Chiba University). The method for the generation of virus supernatant were described previously⁴⁷. FL-DCs were infected with 1:1 ratio viral supernatant:media 48 h after start of Flt3L culture by centrifugation (1800 rpm $750 \times g$, 1 h). Next day, virus was washed from cells and fresh media containing Flt3L was added. Five days after infection, GFP⁺ and GFP⁻ CD11b-DCs were sorted using a BD FACS Aria II flow cytometry. CD11b-DCs were stimulated with media alone or 50ng/ml TSLP for 72 h, supernatants were collected and CCL17 ELISA was performed.

Immunoprecipitation and immunoblotting

FL-CD11b-DCs were stimulated with 50ng/ml of indicated cytokine for indicated times. Cell extracts were prepared using 150mM NaCl lysis buffer containing 1% Triton-X-100 including complete protease and phosphatase inhibitors (Sigma-Aldrich). Cell extracts were resolved by 4–12% BIS TRIS NuPage gel (Invitrogen) and transferred to nitrocellulose membrane (Bio-Rad). The membranes were immunoblotted with anti-phospho-Jak1 (Y1022/1023), anti-total-Jak1, anti-phospho-Jak2 (Y1007/1008), anti-total-Jak2, anti-total-STAT-3 and -5, anti-phospho-STAT-3 (Y705), -5 (Y694), total SOCS-1, -2, and -3 (Cell Signaling), anti-phospho-Jak1 (Y1034/1035). The levels of protein were visualized with HRP-conjugated secondary antibodies by ECL detection system (Millipore). For immunoprecipitation, 2×10^7 cells were cultured in 1% serum containing media for 30 min to reduce background phosphorylation, and anti-total-Jak1 (6G4) and anti-total-Jak2 (D2E12) (Cell Signaling) were used, according to the manufacturer's protocol.

In vitro CD4 cell differentiation cultures

FL-CD11b-DCs were sorted, and cells were stimulated with medium or TSLP (50 ng/ml) for 1 or 2 days. Cells were washed and pulsed with OVA (323–339) (0.01 μ M) for 1 h. Naïve splenic CD4⁺CD62L⁺ T cells (2.5×10^5 cells / ml) from DO11. 10 mice were stimulated in

the presence of medium- or TSLP-treated CD11b-DCs (5×10^4 cells / ml) in 96-round well plate. Residual TSLP was extensively washed off DCs before addition of T cells. For CFSE dilution assay, labeling of the CD4 cells with 5 μ M CFSE (Invitrogen) for 8 min at 37 °C before the co-culture. For the induction of T_H1 cells, IL-2 (25U/ml; eBioscience), IL-12 (1ng/ml; eBioscience), anti-IL-4 (11B11; 1 μ g/ml; National Institute of Health); for the induction of T_H2 cells, IL-2 (25U/ml), IL-4 (0.01–10ng/ml), anti-IFN- γ mAb culture supernatant (R4-6A2) were also added to the culture. On day 3, cells were maintained with IL-2 until day 5. Cells were harvested and washed, and then cells (5×10^4) were stimulated with plate-bound 6 μ g/ml anti-CD3 mAb (2C11) and 8 μ g/ml anti-CD28 mAb (35. 71) (UCSF) for 2 days. Supernatants were collected and ELISA was performed for IL-4, IL-5, IL-13, and IFN- γ as described⁴⁶. The concentration was measured with clones JES5-16E3 and JES5-2A5 (eBioscience) for IL-10. For Intracellular cytokine staining cells, cells were stimulated with plate-bound anti-CD3 mAb (2C11) and anti-CD28 mAb(35. 71)(UCSF) in the presence of Monensin (eBioscience) for 6 h. The Intracellular cytokines were stained using BD Cytofix/Cytoperm Fixation/Permeabilization Kit (BD Biosciences), according to the manufacturer's protocol.

DC isolation

Ears were removed with scissors, split with two pairs of forceps and floated dermis side down in Dispase(3mg/ml or 2.4 U/ml as per manufacturers recommendation) for 1 h at 37 °C (Roche). Langerhans cells and dermal DCs were isolated for FACS analysis by removing epidermis from dermis with two sets of forceps and place each separately) in 50 μ g/ml Liberase for 30 min at 37 °C with shaking. Liberated cells were then washed 3 times in ice cold PBS.

Fluorescent Microscopy

Epidermal sheets were separated from the dermal layer through dispase digestion at 37 °C for 1 h (Roche). Epidermis was washed three times in PBS, fixed with ice-cold methanol for 15 min at -20 °C, washed two times in PBS, and rehydrated in PBS for 30 min at room temperature(15 to 25 °C). Epidermis was then blocked with PBS (1% BSA, 0.1% Tween-20) two times, followed by overnight incubation with anti-MHCII-FITC, 1:200 in blocking buffer at 4 °C. Epidermis was washed 5 more times the following day, followed by mounting on glass slides with vectashield:DAPI (vector labs) and imaged on ICL DMIRB inverted scope.

Intradermal injections

Mice were intravenously injected with CFSE labeled DO11 naïve CD4⁺ T cells. 4 h later, mice were given intradermal injections on the shaved back with 5 μ g of OVA plus or minus 5 μ g of TSLP in PBS. Seven days later, pooled skin dLNs were restimulated with PMA and ionomycin for 4 h in the presence of monensin.

Contact Hypersensitivity

CHS was induced in mice using the hapten fluorescein isothiocyanate (FITC) or dinitrofluorobenzene (DNFB). FITC was resuspended in 1:1 acetone and dibutyl phthalate

(DBP) to a concentration of 0.5%. DNFB was diluted in 4:1 acetone and olive oil to a concentration of 0.5%. On day 0 mice were sensitized with 100 μ l 0.5% FITC or vehicle (1:1 DBP/acetone) for the FITC model; or with 50 μ l 0.5% DNFB or vehicle (4:1 acetone/olive oil) for the DNFB model. On day 6, baseline ear thickness was measured with calipers followed by challenging the mice on one ear with 20 μ l of 0.5% hapten and vehicle on the contralateral ear. On day 7, 24 h post-challenge, ear thickness was measured to calculate the change in ear thickness. In some experiments hapten-sensitized mice were injected i. p. with BrdU 1 mg/day on days 1 through 5.

ELISA

FL-DCs (2×10^5) were stimulated with medium alone or medium plus TSLP (50 ng/ml) for 3 days. The production of CCL17 was measured using a mouse CCL17 ELISA Kit (R&D Systems), according to the manufacturer's protocol.

Influenza virus A Infection, tissue preparation and analysis

Mice were lightly anesthetized with ketamine (100 mg/kg) and xylazine (1 mg/kg) and then intranasally infected with Influenza A virus X-31 (A/Aichi/68 (H3N2); 5×10^3 TCID₅₀) in 30 μ l of PBS. At the specified times mice were euthanized by lethal injection with 1 ml of 2.5% Avertin in PBS i. p. The lungs were subjected to BAL five times, each with 1 ml of PBS through a tracheal cannula, followed by cardiac perfusion with 10 ml PBS. BAL cells were pelleted and resuspended in RPMI 1640/5% FCS/HEPESpH 7.4/pen-strep/glutamine. Lung and mediastinal lymph nodes (mLN) were minced into small pieces and incubated with collagenase buffer (RPMI 1640/2% FCS/HEPES pH 7.4/pen-strep/glutamine/e/CaCl₂/MgCl₂, and collagenase [100 U/ml; Invitrogen]) for 1 h (lung) or 30 min (mLN) at 37 °C under agitation. At the end of incubation, remaining tissue pieces were crushed through 100- μ m nylon mesh filter (BD Biosciences). The resulting mLN cells were pelleted and resuspended in RPMI 1640/5% FCS/HEPESpH 7.4/pen-strep/glutamine, while the resulting lung cells were pelleted and resuspended in 44% Percoll buffer (GE Life Sciences) and underlain with 67% Percoll buffer. Percoll gradients were centrifuged at $1700 \times g$, and cells at the Percoll gradient interface were extracted, washed, and resuspended in RPMI 1640/5% FCS/HEPESpH 7.4/pen-strep/glutamine. For staining, lymphocytes were suspended in PBS/0.2% BSA/0.1% NaN₃ (FACS buffer) at a concentration of $2 \times 10^6/50 \mu$ l and stained with the appropriate antibodies at 4°C for 20 min, washed, and fixed in PBS with 2% paraformaldehyde. For tetramer staining cells were incubated with tetramer (NP₁₄₇₋₁₅₅/H-2K^d) (NIH Tetramer Core Facility, Atlanta, GA) and the appropriate antibodies at room temperature (15 to 25 °C) for 1 h, washed, and fixed in PBS with 2% paraformaldehyde. For *in vitro* T cell restimulation assays, 2×10^6 cells from mLN or lung were resuspended in 200 μ l of RPMI 1640/5% FCS/HEPESpH 7.4 /pen-strep/glutamine containing 50 ng/ml phorbol 12-myristate 13-acetate, 750 ng/ml ionomycin and 10 μ g/ml brefeldin and incubated for 4 h at 37°C 5% CO₂ in a 96-well plate. After stimulation, cells were washed with FACS buffer and stained for surface molecules overnight at 4°C, then fixed and permeabilized in Cytofix/Cytoperm solution (BD Pharmingen). Cells were stained with anti-cytokine antibodies or their respective isotype controls. Samples were acquired on a LSR II (BD Biosciences). Data were analyzed using FlowJo Software (Tree Star).

Statistical analysis

The significance between two groups was determined by two-tailed Student's *t* test, and one- or two-way ANOVA.

Supplementary Material

Refer to Web version on PubMed Central for supplementary material.

Acknowledgements

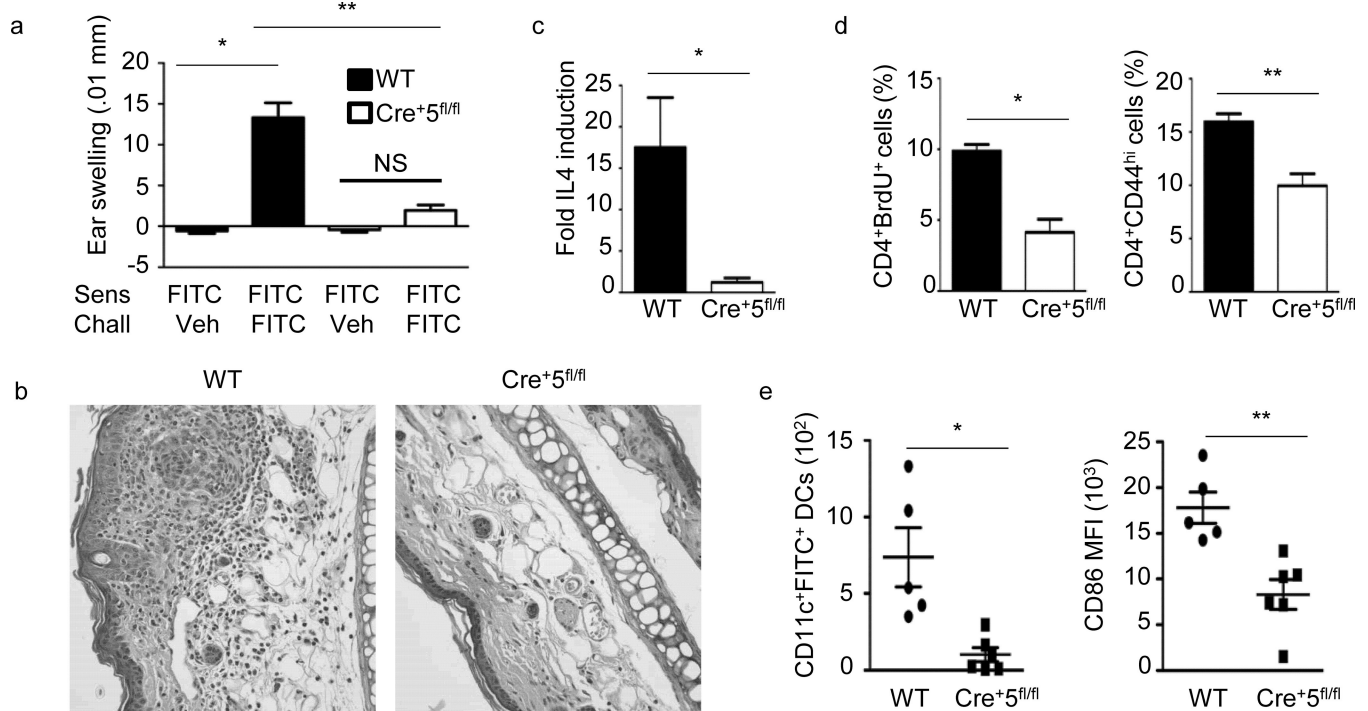
We thank D. Rawlings and H. Kerns for providing reagents. We thank J. Hamerman and D. Campbell for critical discussion of the manuscript and S. Ma and W. Xu for their technical support. We also thank M. Warren and S. McCarty for their administrative support. The work was supported in part by NIH grants R01-AI068731, R01-AR056113, R01-AR055695, and P01-HL098067 (S. F. Z.). B. D. B. is supported by training grant 5T32AI007411-19.

Reference List

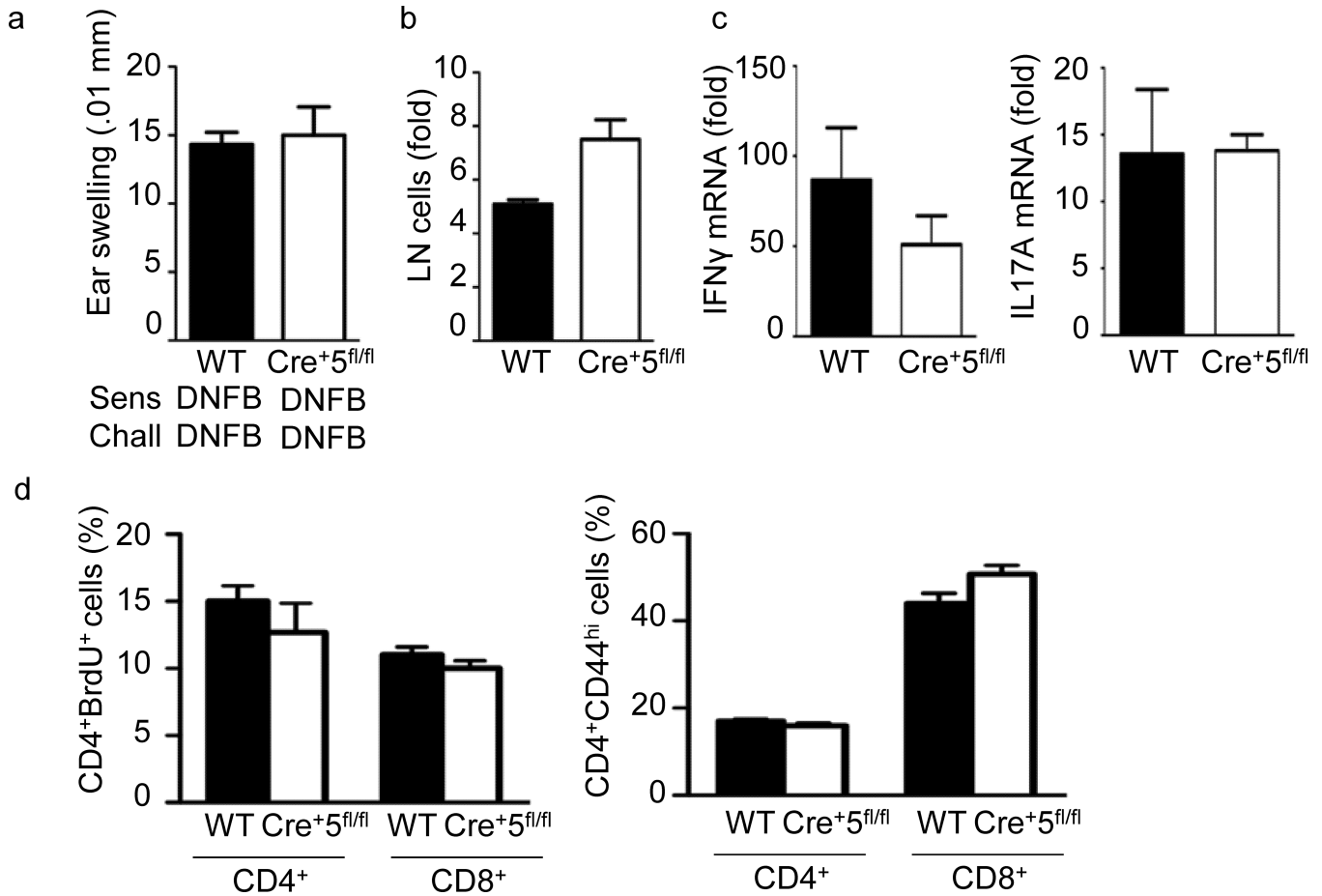
- Shortman K, Naik SH. Steady-state and inflammatory dendritic-cell development. *Nat Rev Immunol.* 2007; 7:19–30. [PubMed: 17170756]
- McKenna HJ, et al. Mice lacking flt3 ligand have deficient hematopoiesis affecting hematopoietic progenitor cells, dendritic cells, and natural killer cells. *Blood.* 2000; 95:3489–3497. [PubMed: 10828034]
- Laouar Y, Welte T, Fu XY, Flavell RA. STAT3 is required for Flt3L-dependent dendritic cell differentiation. *Immunity.* 2003; 19:903–912. [PubMed: 14670306]
- Onai N, Obata-Onai A, Tussiwand R, Lanzavecchia A, Manz MG. Activation of the Flt3 signal transduction cascade rescues and enhances type I interferon-producing and dendritic cell development. *J Exp Med.* 2006; 203:227–238. [PubMed: 16418395]
- Esashi E, et al. The signal transducer STAT5 inhibits plasmacytoid dendritic cell development by suppressing transcription factor IRF8. *Immunity.* 2008; 28:509–520. [PubMed: 18342552]
- Schiavoni G, et al. ICSBP is essential for the development of mouse type I interferon-producing cells and for the generation and activation of CD8alpha(+) dendritic cells. *J Exp Med.* 2002; 196:1415–1425. [PubMed: 12461077]
- Zenke M, Hieronymus T. Towards an understanding of the transcription factor network of dendritic cell development. *Trends Immunol.* 2006; 27:140–145. [PubMed: 16406699]
- Ziegler SF, Artis D. Sensing the outside world: TSLP regulates barrier immunity. *Nat Immunol.* 2010; 11:289–293. [PubMed: 20300138]
- Liu YJ, et al. TSLP: an epithelial cell cytokine that regulates T cell differentiation by conditioning dendritic cell maturation. *Annu Rev Immunol.* 2007; 25:193–219. [PubMed: 17129180]
- Rochman Y, et al. Thymic stromal lymphopoietin-mediated STAT5 phosphorylation via kinases JAK1 and JAK2 reveals a key difference from IL-7-induced signaling. *Proc. Natl. Acad. SciUS.A.* 2010; 107:19455–19460.
- Arima K, et al. Distinct signal codes generate dendritic cell functional plasticity. *Sci. Signal.* 2010; 3:ra4. [PubMed: 20086239]
- Isaksen DE, et al. Requirement for stat5 in thymic stromal lymphopoietin-mediated signal transduction. *J Immunol.* 1999; 163:5971–5977. [PubMed: 10570284]
- Levin SD, et al. Thymic stromal lymphopoietin: a cytokine that promotes the development of IgM + B cells in vitro and signals via a novel mechanism. *J. Immunol.* 1999; 162:677–683. [PubMed: 9916685]
- Isaksen DE, et al. Uncoupling of proliferation and Stat5 activation in thymic stromal lymphopoietin-mediated signal transduction. *J Immunol.* 2002; 168:3288–3294. [PubMed: 11907084]

15. Rochman Y, Spolski R, Leonard WJ. New insights into the regulation of T cells by gamma(c) family cytokines. *Nat. Rev. Immunol.* 2009; 9:480–490. [PubMed: 19543225]
16. Kitajima M, Lee HC, Nakayama T, Ziegler SF. TSLP enhances the function of helper type 2 cells. *Eur. J. Immunol.* 2011; 41:1862–1871. [PubMed: 21484783]
17. Al Shami A, Spolski R, Kelly J, Keane-Myers A, Leonard WJ. A role for TSLP in the development of inflammation in an asthma model. *J. Exp. Med.* 2005; 202:829–839. [PubMed: 16172260]
18. He R, et al. TSLP acts on infiltrating effector T cells to drive allergic skin inflammation. *Proc. Natl. Acad. SciUS.A.* 2008; 105:11875–11880.
19. Larson RP, et al. Dibutyl phthalate-induced thymic stromal lymphopoietin is required for th2 contact hypersensitivity responses. *J Immunol.* 2010; 184:2974–2984. [PubMed: 20173025]
20. Soumelis V, et al. Human epithelial cells trigger dendritic cell mediated allergic inflammation by producing TSLP. *Nat. Immunol.* 2002; 3:673–680. [PubMed: 12055625]
21. Henri S, et al. Disentangling the complexity of the skin dendritic cell network. *Immunol. Cell Biol.* 2010; 88:366–375. [PubMed: 20231850]
22. Merad M, Manz MG. Dendritic cell homeostasis. *Blood.* 2009; 113:3418–3427. [PubMed: 19176316]
23. Melillo JA, et al. Dendritic cell (DC)-specific targeting reveals Stat3 as a negative regulator of DC function. *J Immunol.* 2010; 184:2638–2645. [PubMed: 20124100]
24. Takeshita K, Yamasaki T, Akira S, Gantner F, Bacon KB. Essential role of MHC II-independent CD4+ T cells, IL-4, and STAT6 in contact hypersensitivity induced by fluorescein isothiocyanate in the mouse. *Int. Immunol.* 2004; 16:685–695. [PubMed: 15096484]
25. Dearman RJ, Kimber I. Role of CD4(+) T helper 2-type cells in cutaneous inflammatory responses induced by fluorescein isothiocyanate. *Immunology.* 2000; 101:442–451.
26. Gorbachev AV, Fairchild RL. Induction and regulation of T-cell priming for contact hypersensitivity. *Crit Rev. Immunol.* 2001; 21:451–472. [PubMed: 11942559]
27. Bobr A, et al. Acute ablation of Langerhans cells enhances skin immune responses. *J Immunol.* 2010; 185:4724–4748. [PubMed: 20855870]
28. Zhou B, et al. Thymic stromal lymphopoietin as a key initiator of allergic airway inflammation in mice. *Nat. Immunol.* 2005; 6:1047–1053. [PubMed: 16142237]
29. Headley MB, et al. TSLP conditions the lung immune environment for the generation of pathogenic innate and antigen-specific adaptive immune responses. *J. Immunol.* 2009; 182:1641–1647. [PubMed: 19155513]
30. Taylor BC, et al. TSLP regulates intestinal immunity and inflammation in mouse models of helminth infection and colitis. *J. Exp. Med.* 2009; 206:655–667. [PubMed: 19273626]
31. Ito T, et al. TSLP-activated dendritic cells induce an inflammatory T helper type 2 cell response through OX40 ligand. *J. Exp. Med.* 2005; 202:1213–1223. [PubMed: 16275760]
32. Ziegler SF. The role of thymic stromal lymphopoietin (TSLP) in allergic disorders. *Curr Opin Immunol.* 2010; 22:795–799. [PubMed: 21109412]
33. Alferink J, et al. Compartmentalized production of CCL17 in vivo: Strong inducibility in peripheral dendritic cells contrasts selective absence from the spleen. *J Exp Med.* 2003; 197 :585–599. [PubMed: 12615900]
34. Caton ML, Smith-Raska MR, Reizis B. Notch-RBP-J signaling controls the homeostasis of CD8-dendritic cells in the spleen. *J. Exp. Med.* 2007; 204:1653–1664. [PubMed: 17591855]
35. Birnberg T, et al. Lack of conventional dendritic cells is compatible with normal development and T cell homeostasis, but causes myeloid proliferative syndrome. *Immunity.* 2008; 29:986–997. [PubMed: 19062318]
36. Ohnmacht C, et al. Constitutive ablation of dendritic cells breaks self-tolerance of CD4 T cells and results in spontaneous fatal autoimmunity. *J Exp Med.* 2009; 206:549–559. [PubMed: 19237601]
37. Yoo J, et al. Spontaneous atopic dermatitis in mice expressing an inducible thymic stromal lymphopoietin transgene specifically in the skin. *J. Exp. Med.* 2005; 202:541–549. [PubMed: 16103410]

38. Li M, et al. Topical vitamin D3 and low-calcemic analogs induce thymic stromal lymphopoietin in mouse keratinocytes and trigger an atopic dermatitis. *Proc. Natl. Acad. SciUS.A.* 2006; 103:11736–11741.
39. Briot A, et al. Kallikrein 5 induces atopic dermatitis-like lesions through PAR2-mediated thymic stromal lymphopoietin expression in Netherton syndrome. *J. Exp. Med.* 2009; 206:1135–1147. [PubMed: 19414552]
40. Dumortier A, et al. Atopic dermatitis-like disease and associated lethal myeloproliferative disorder arise from loss of notch signaling in the murine skin. *PLoS. ONE.* 2010; 5:e9258. [PubMed: 20174635]
41. Luche H, Weber O, Nageswara-Rao T, Blum C, Fehling HJ. Faithful activation of an extra-bright red fluorescent protein in "knock-in" Cre-reporter mice ideally suited for lineage tracing studies. *Eur J Immunol.* 2007; 37 :43–53. [PubMed: 17171761]
42. Cui Y, et al. Inactivation of Stat5 in Mouse Mammary Epithelium during Pregnancy Reveals Distinct Functions in Cell Proliferation, Survival, and Differentiation. *Mol Cell Bio.* 2004; 24:8037–8047. [PubMed: 15340066]
43. Kaplan DH, Jenison MC, Saeland S, Shlomchik WD, Shlomchik MJ. Epidermal Langerhans cell-deficient mice develop enhanced contact hypersensitivity. *Immunity.* 2005; 23:611–620. [PubMed: 16356859]
44. Murphy KM, Heimberger AB, Loh DY. Induction by antigen of intrathymic apoptosis of CD4⁺CD8⁺ TCR^{lo} thymocytes in vivo. *Science.* 1990; 250:1720–1723. [PubMed: 2125367]
45. Lutz MB, et al. An advanced culture method for generating large quantities of highly pure dendritic cells from mouse bone marrow. *J Immunological Methods.* 1999; 223:77–92. [PubMed: 10037236]
46. Omori M, Ziegler S. Induction of IL-4 expression in CD4(+) T cells by thymic stromal lymphopoietin. *J Immunol.* 2007; 178:1396–1404. [PubMed: 17237387]
47. Bell BD, et al. FADD and caspase-8 control the outcome of autophagic signaling in proliferating T cells. *Proc Natl Acad Sci U S A.* 2008; 16682

**Figure 1.**

T_H2-type CHS is significantly reduced in Cre^{+5fl/fl} mice. **(a)** Mice were sensitized on the abdomen with 0.5% FITC on day 0, baseline ear thickness was measured on day 6, followed by challenge with FITC or vehicle. Change in ear thickness was measured 24 h post-challenge. WT is BALB/c control mice. * = .0001, ** = .0003. **(b)** Representative of five H&E-stained ear sections fixed 24 h post-challenge from WT and Cre^{+5fl/fl} mice sensitized and challenged with FITC. **(c)** Ear tissue was excised and processed 24 h after challenge. IL-4 mRNA fold induction is relative to the WT vehicle-challenged samples and normalized to HPRT. * = .024 **(d)** Percent of CD4⁺ T cells positive for BrdU or CD44 from skin draining LNs 24 h following challenge. * = .005, ** = .012 **(e)** Number of CD11c⁺FITC⁺ DCs and the MFI of CD86 on the CD11c⁺FITC⁺ DCs in axillary and inguinal LNs 24 h post-sensitization on the abdomen with 0.5% FITC. Representative of 5 independent experiments with 4–6 mice per group, +/-SEM. * = .049, ** = .005.

**Figure 2.**

Normal T_H1-type CHS in Cre⁺⁵^{fl/fl} mice. (a) Mice were sensitized with DNFB on the abdomen on day 0, baseline ear thickness was measured on day 6, followed by challenge with DNFB on the ear. Change in ear thickness was measured 24 h post-challenge. (b) Fold change in pooled axillary and inguinal LN cellularity from WT(BALB/c) and Cre⁺⁵^{fl/fl} mice following challenge compared to non-sensitized, non-challenged mice. (c) Ear tissue was excised and processed 24 h after challenge. mRNA fold induction is relative to the WT vehicle-challenged samples and normalized to HPRT. (d) Percent of CD4⁺ T cells positive for BrdU or CD44 from skin dLNs 24 h following challenge. CHS results are representative of three independent experiments with 4–5 mice per group, +/-SEM.

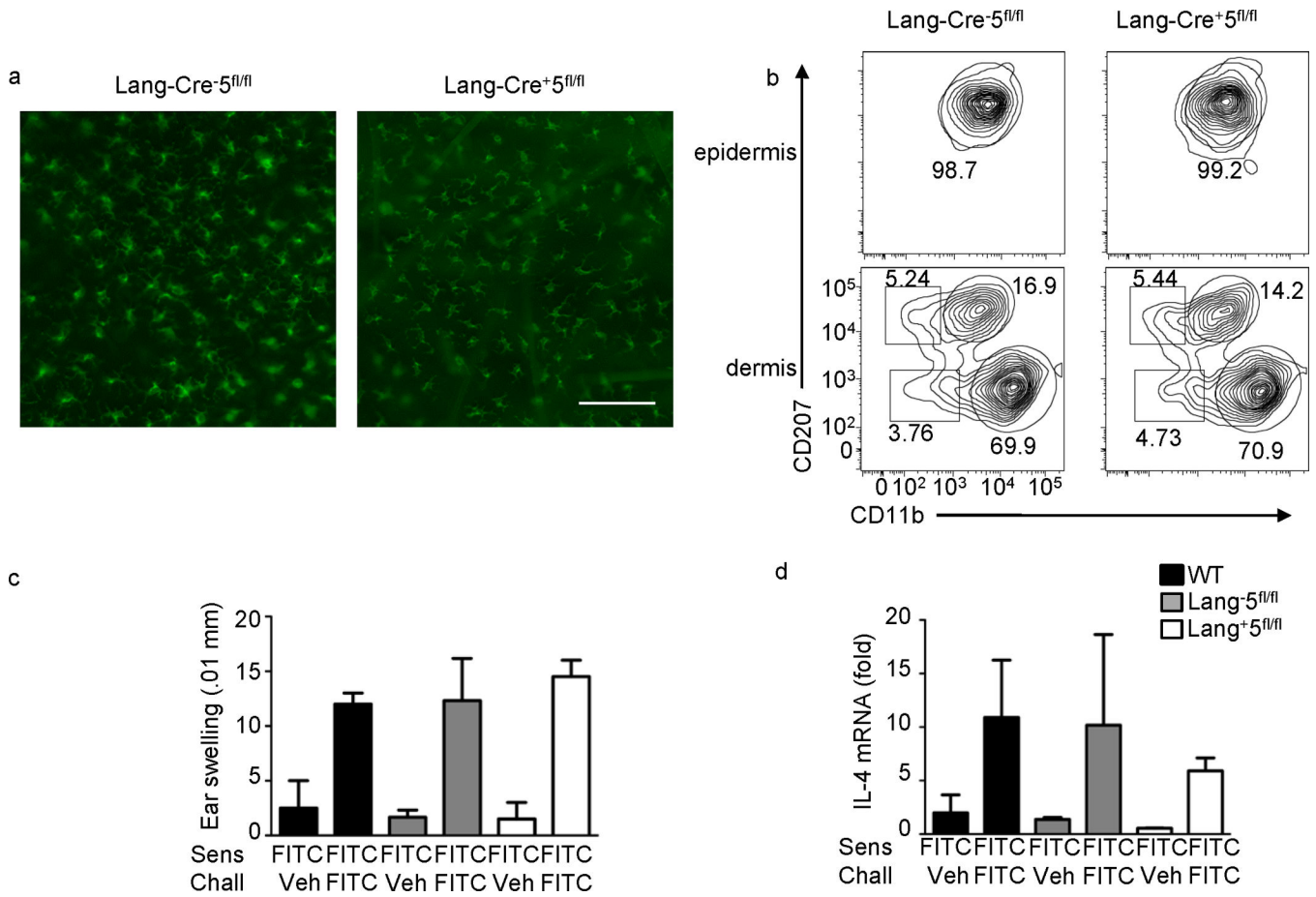
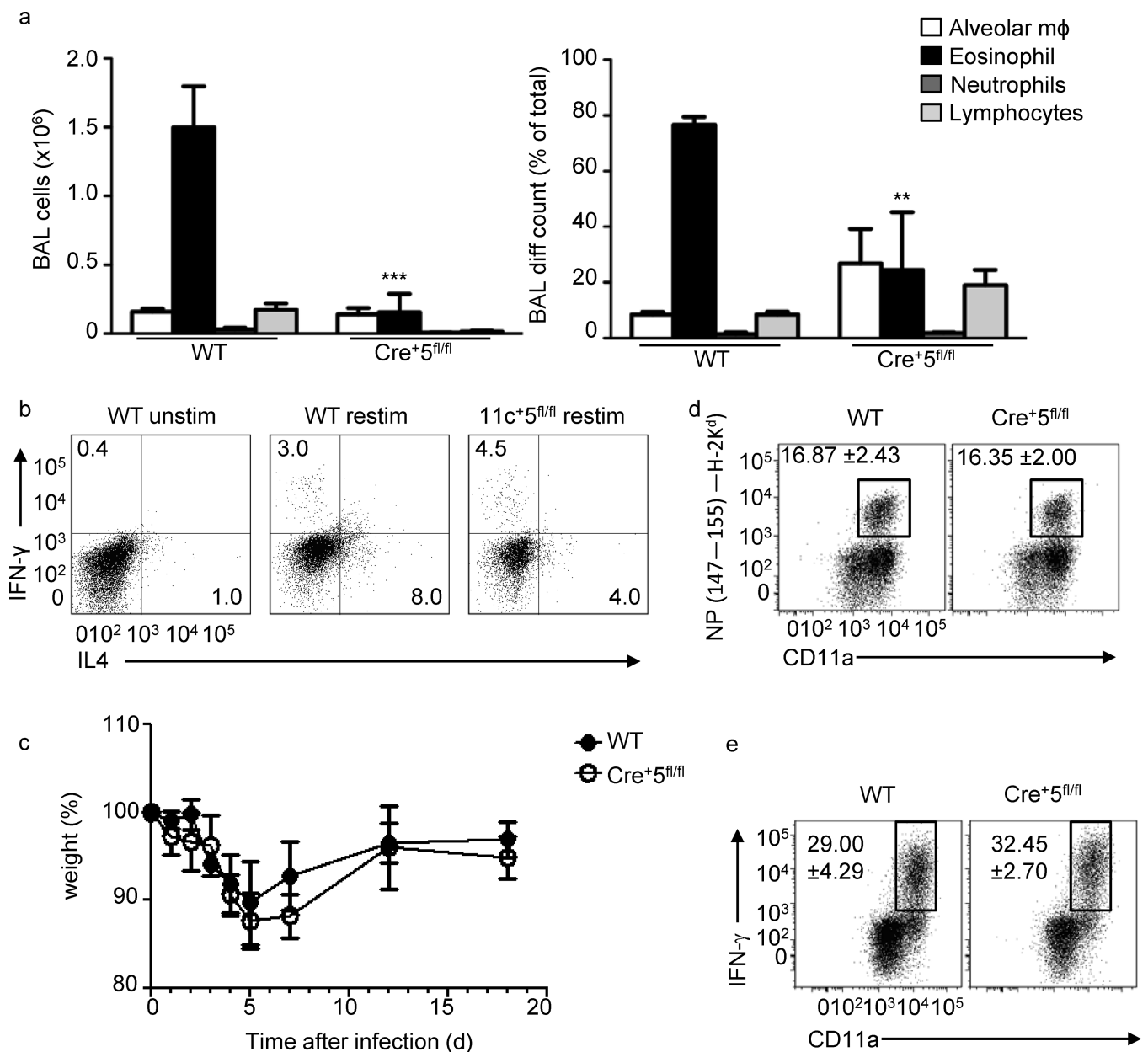


Figure 3. STAT5 is not required in Langerhans cells for T_H2-type CHS. **(a)**Fluorescent microscopy for MHCII in epidermal sheets from *Lang-Cre⁻* and *Lang-Cre⁺ STAT5^{fl/fl}* ears. Scale bar is 100 μm, representative of 5 independent mice. **(b)**MHCII⁺ cells were analyzed for the expression of CD207 (langerin) and CD11b in the epidermis and dermis of *Cre⁻STAT5^{fl/fl}* and *Cre⁺STAT5^{fl/fl}* mice. Graphs and percentages are representative of three independent experiments. **(c)** Mice were sensitized on the abdomen with 0.5% FITC on day 0, baseline ear thickness was measured on day 6, followed by challenge with FITC or vehicle. Change in ear thickness was measured 24 hours post-challenge. WT is BALB/c control mice. **(d)** Ear tissue was excised and processed 24 hours after challenge. IL-4 mRNA fold induction is relative to the WT vehicle-challenged samples and normalized to HPRT. Representative of three independent experiments with 3–4 mice per group.

**Figure 4.**

T_H2 -, but not T_H1 -type immune responses in the lung require STAT5 in DCs. (a) Mice were sensitized with OVA-alum on day 0, followed by intranasal challenge with OVA on days 7–9, and analyzed on day 10. BAL cell number and percent of each cell population (are average of three mice per experiment. * = .0001 (b) mLNNT cells were restimulated for 4 h, followed by intracellular cytokine staining for IL-4, IL-13 and IFN- γ . ** = .0005. Wild-type and Cre^{+5fl/fl} mice were intranasally infected with Influenza A/Aichi/68 (H3N2; 5×10^3 TCID₅₀) and (c) their weight loss was tracked as a read out of pathology. On day 8 post-infection a cohort of wild-type and Cre^{+5fl/fl} mice were analyzed for their (d) antigen-specific CD8⁺ T cell response using the NP_{147–155}/H-2K^d tetramer and (e) the percentage of

influenza stimulated CD4⁺ T cells capable of producing IFN- γ after *in vitro* restimulation with PMA and ionomycin (see **Methods**).

Author Manuscript

Author Manuscript

Author Manuscript

Author Manuscript

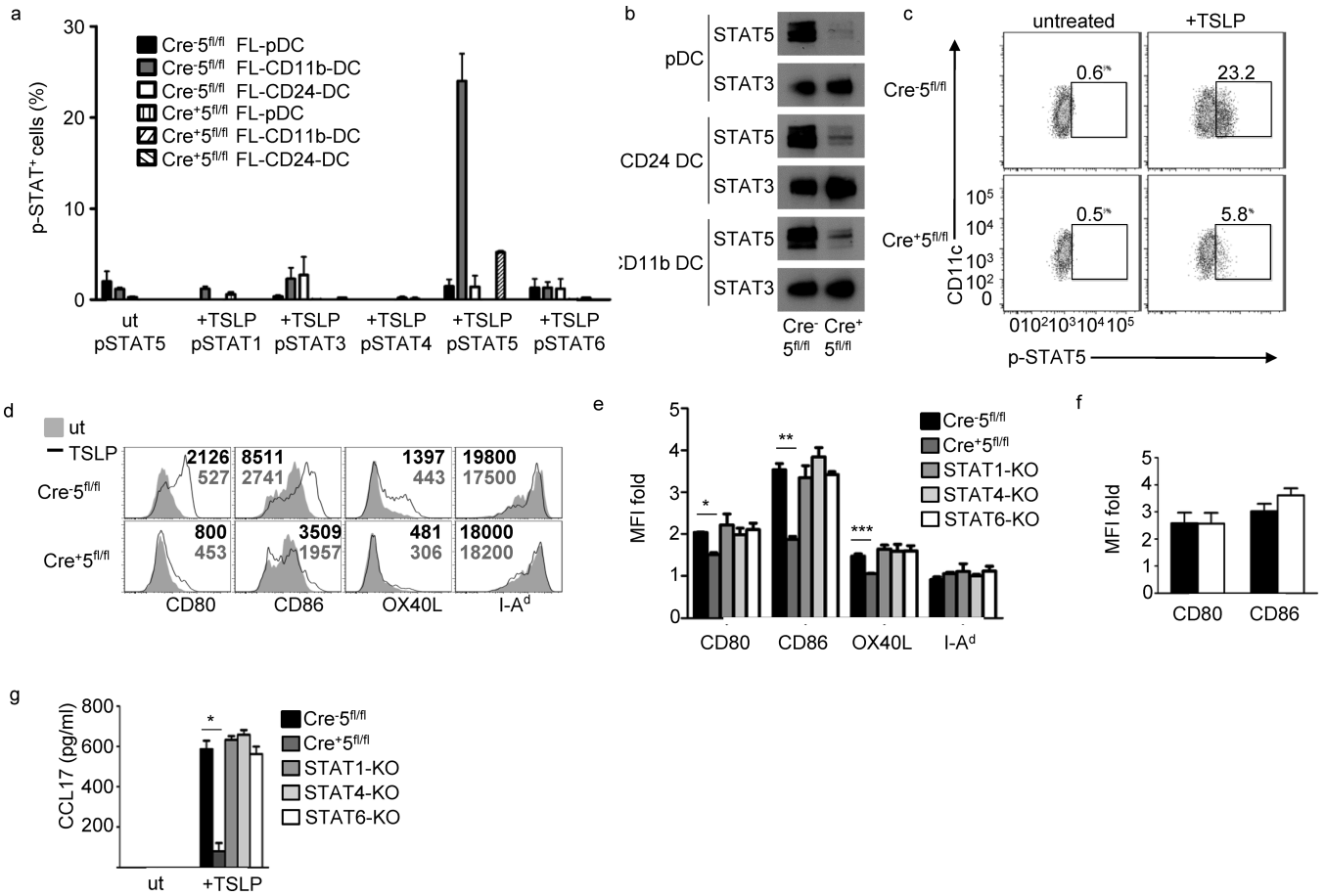


Figure 5.

Representative of 2 experiments with 5 mice per group. Figure 5 STAT5 is required for TSLP-induced costimulatory molecule upregulation in FL-CD11b-DCs. **(a)** Phospho-Flow of indicated STAT proteins in three FL-DC populations, in triplicate, following 15 min incubation with 50ng/ml TSLP from WT (Cre⁻5^{fl/fl}) and Cre⁺5^{fl/fl} BMDCs. Three independent experiments. **(b)** Immunoblot of total-STAT5 and -STAT3 in FL-DC populations. **(c)** pSTAT5 phospho-flow of WT and Cre⁺5^{fl/fl} FL-CD11b-DC following 15 min incubation with TSLP. **(d)** Costimulatory molecule expression in TSLP-treated and – untreated FL-CD11b-DCs. Numbers represent MFI values. **(e)** Fold-change of TSLP-treated versus untreated FL-CD11b-DCs from WT, Cre⁺5^{fl/fl}, STAT-1, -4, and -6 KO bone marrow in triplicate, 4 independent experiments. * = .01, ** = .0005, *** = .05 **(f)** Fold change of costimulatory molecule upregulation in WT (black bar) and Cre⁺5^{fl/fl} (white bar) following LPS stimulation in triplicate. **(g)** Expression of CCL17 in FL-CD11b-DCs from e. * = .00003.

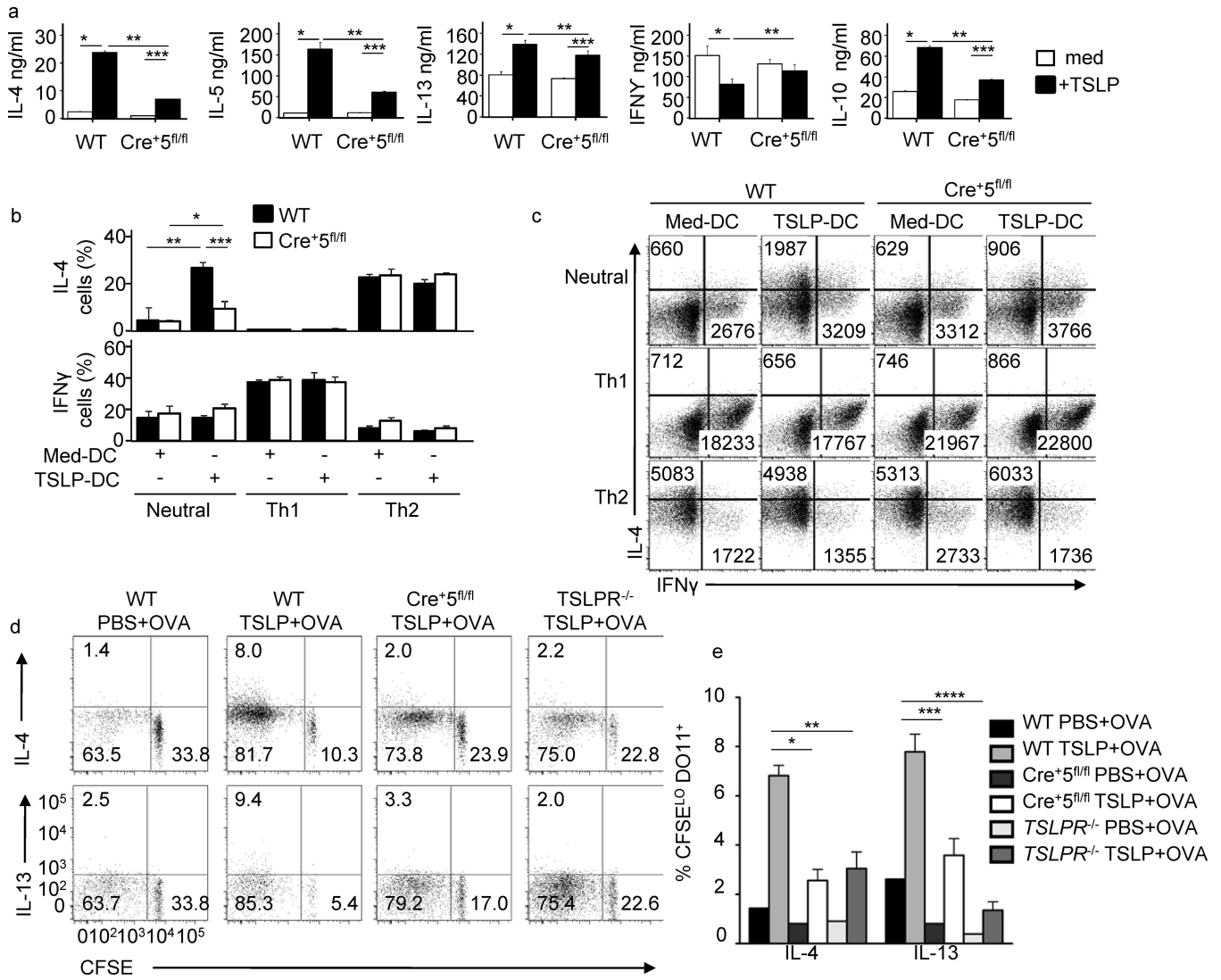


Figure 6. TSLP-induced STAT5 in DCs is required for TH2 differentiation of CD4+ T cells. (a) DO11.10 CD4+ T cells were cocultured with OVA(323–339)-pulsed (0.01 μM) TSLP-pretreated or untreated Cre-5fl/fl and Cre+5fl/fl FL-CD11b-DCs. DCs were treated overnight with TSLP, followed by extensive washing to remove residual TSLP before addition of T cells. T cells were stimulated for 5 days, followed by ELISA for indicated cytokines. **P* < 0.05 and ***P* < 0.01 (one-way ANOVA). (b, c) Percent CD4+ T cells positive for IL-4 and IFN-γ (b, bar graphs) and average MFI for x and y axis separately. **P* < 0.05 and ***P* < 0.01 (one-way ANOVA). c, numbers in FACS plots after coculture with TSLP-pretreated and untreated Cre-5fl/fl and Cre+5fl/fl FL-CD11b-DCs in neutral, TH1 and TH2 skewing conditions, measured by flow cytometry. (d) WT, Cre+5fl/fl and TSLPR-/- were intravenously injected with CFSE labeled DO11.10 naïve CD4+ T cells. Mice were given intradermal injections of OVA plus or minus TSLP in PBS. Seven days later, pooled skin dLNs were restimulated and intracellular cytokine staining for IL-13 and IL-4 was detected by flow cytometry and graphed relative to CFSE dilution. Representative of four mice per

group, two independent experiments. (e) Percent of CFSE¹⁰DO11.10⁺ T cells from (d) positive for IL-4 or IL-13. * = .002, ** = .003, *** = .001, **** = .0003.

Author Manuscript

Author Manuscript

Author Manuscript

Author Manuscript